Available online at www.sciencedirect.com
ScienceDirect
Journal of Organometallic Chemistry 693 (2008) 639–645
Journal of Organometallic Chemistry
www.elsevier.com/locate/jorganchem

Bonding analysis and the mechanisms on the ring-opening of alkoxy-bridged bis(silylene) transition-metal complexes toward MeOH

Siwei Bi [a,c,*], Yanyun Zhao [a,b], Xiaojian Kong [a], Xiaoran Zhao [a], Qingming Xie [a]

[a] College of Chemistry Science, Qufu Normal University, Qufu, Shandong 273165, China
[b] Department of Chemistry, TaiShan University, Tai'an, Shandong 271021, China
[c] Key Laboratory of Colloid and Interface Chemistry, Shandong University, Ministry of Education, Jinan, Shandong 250100, China

Received 24 October 2007; received in revised form 21 November 2007; accepted 27 November 2007
Available online 4 December 2007

Abstract

The mechanistic study on the ring-opening of alkoxy-bridged bis(silylene) transition-metal complexes toward MeOH is performed by using density functional theory. Four steps are predicted to be involved in the reaction, formation of hydrogen bonding between **R** and a MeOH, ring-opening of the Ru–Si1–O1–Si2 four-membered ring, formation of the six-membered ring, and the hydroxyl hydrogen migration to the metal center. It is found that the reaction is favorable thermodynamically and the hydroxyl hydrogen migration is the rate-determining step. Systematic variations of the structural parameters involved in the reaction mechanism are revealed, which revealed the relationship of the bond strength among Ru–Si, Si–O and O–H bonds.

Keywords: Alkoxy-bridged bis(silylene) complex; Ring-opening; Reaction mechanism; Density functional calculation

1. Introduction

Donor-stabilized silylene transition-metal complexes are considered to play an important role in many metal-catalyzed transformations of organosilicon compounds. The first two reports about successful syntheses of donor-stabilized silylene complexes were reported by Tilley and Straus [1] and Zybill and Muller [2]. In 1988, Ogino group [3] have successfully synthesized and characterized the first intramolecular donor-bridged bis(silylene)iron complex, and a series donor-bridged bis(silylene) transition-metal complexes [4–7] were synthesized in the following years, as shown in Scheme 1.

Among these donor-bridged complexes, alkoxy-bridged bis(silylene) transition-metal complexes, with peculiar bond modes and novel reactivity, occupy a unique position in these systems. To our knowledge, transition-metal complexes with silylene or silyl ligands have been analyzed in a variety of theoretical studies [8–14], but few detailed theoretical studies are focused on donor-bridged bis(silylene) transition-metal complexes [15,16]. The silicon atom is expected to be vulnerable to various nucleophiles such as ROH, RCN, and H_2O [17–21]. This kind of nucleophilic reactions should be one of the most common reactions of silylene complexes. In this paper, we choose a representative reaction system of $CpRu(CO)SiMe_2SiMe_2OCH_3$ (**R**) with MeOH to theoretically investigate the related reaction mechanism and bonding properties [22] (see reaction 1). Our aim is that this work can be expected to present deep understanding for this kind of reactions.

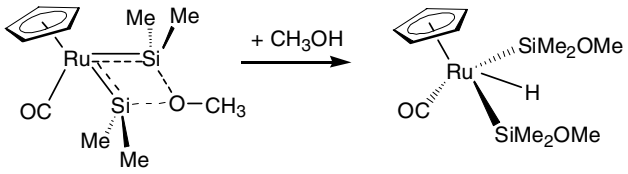

* Corresponding author. Address: College of Chemistry Science, Qufu Normal University, Qufu, Shandong 273165, China. Fax: +86 537 4456305.
E-mail address: siweibi@126.com (S. Bi).

0022-328X/$ - see front matter © 2007 Elsevier B.V. All rights reserved.
doi:10.1016/j.jorganchem.2007.11.044

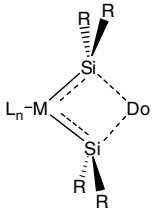

Scheme 1. (a) (M = Fe, Ru; Do = OR, NR_2) [4]; (b) (M = Mn; Do = OR) [5]; (c) (M = Mo,Cr; Do = OR, NR_2) [6]; and (d) (M = W, Do = OR, NR_2) [7], etc.

2. Computational details

Molecular geometries of all complexes in this work were optimized without any constraints at the Becke3LYP (B3LYP) [23] level of density functional theory [24,25]. Frequency calculations at the same level have also been performed to identify all the stationary points as minima (zero imaginary frequency) or transition states (one imaginary frequency). The effective core potentials (ECPs) of Hay and Wadt with a double-ζ basis set (LanL2DZ)[26,27] were used to describe Ru, Si atoms. The standard 6-31G [28–30] basis set [31] was used for H, C and O atoms. Polarization functions [32] were also added for Si ($\zeta d = 0.262$), O ($\zeta d = 0.8$), and those atoms directly involved in bond-forming and bond-breaking processes, C ($\zeta d = 0.8$), H ($\zeta d = 0.11$). The transition states involved were checked by calculations of intrinsic reaction coordinates (IRC) [33,34] analysis to confirm that such structures are indeed connecting two minima. All calculations were performed with the GAUSSIAN 98 software package [35]. The methods employed in this work are reliable as reported by literatures [36,37]. We have also used these methods successfully to study some organometallic systems [38–43]. For examining the methods used in this work, the computational structural parameters are compared with the experimental data [22] as shown in Scheme 2. The computational structural parameters are well in accord with the experimental ones, indicating the method is reliable in investigating organosilicon transition-metal systems. Molecular orbitals obtained from the B3LYP calculations were plotted using the MOLDEN v3.5 program written by Schaftenaar [43].

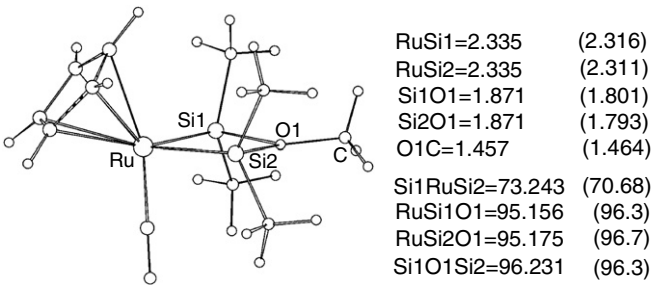

Scheme 2. Calculated geometrical parameters for reactant **R** along with the corresponding parameters from the original X-ray structure (in brackets). Bond lengths are given in Å and bond angles are given in degree.

3. Result and discussion

Experiments confirmed that Cp(OC)Ru{$SiMe_2$(OMe)-$SiMe_2$} (**R**) reacts with MeOH to afford the product Cp(OC)Ru(H)($SiMe_2OMe$)$_2$ (**P**) cleanly [22]. For exploring the mechanism of the reaction and the bonding features, the potential energy profile for formation of Cp(CO)Ru(H)($SiMe_2OMe$)$_2$ from **R** and MeOH has been done and shown in Fig. 1. All the optimized geometrical structures with selected structural parameters are illustrated in Fig. 2.

3.1. Reaction mechanism

The reactant **R** is featured by a coplanar four-membered Ru–Si1–O1–Si2 ring. The two Ru–Si and two Si–O bond distances are calculated to be identical, respectively, which can be rationalized by the structural resonance involved in the four-membered silametallacycle as shown in Scheme 3. The Ru–Si bond distances are calculated to be 2.34 Å, which lies in between the single and the double Ru–Si bond distances. As shown in **Int2**, the single Ru–Si2 bond is calculated to be 2.42 Å and the double bond Ru–Si1 is 2.25 Å. The Si–O bond in **R** is calculated to be 1.87 Å, larger than the Si–O σ-bond distance (~1.70 Å, as illustrated in the geometry of **P**), which can be rationalized from Scheme 3 where the Si–O bond has partial dative-bond character. In addition, the Si1–O1–Si2–C dihedral angle is calculated to be 170.0°, indicating that the O1 atom has almost sp^2 hybridization. The p orbital with a lone pair of electrons on O1, perpendicular to the plane formed by the four atoms, is believed to have π interaction with silicon d orbitals, slightly enhancing the Si–O bond strength. As the lone pair on the p orbital of O1 interacts with hydroxyl hydrogen of MeOH as shown in **Int1**, the π interaction between the p orbital on O1 and the d orbitals on silicon would be reduced and consequently the Si–O bond distances are slightly elongated (1.87 Å in **R** and 1.90 Å in **Int1**).

The first step (**R** to **Int1**) is proposed to be the attack of the MeOH proton to the bridged OMe oxygen. A more stable intermediate **Int1** is formed, in which the hydrogen bonding between the donor O and the MeOH proton is present. The driving force for the step is the formation of the hydrogen bonding. Following this step and through the subsequent steps, the MeOH proton is placed in between the two $SiMe_2$ groups as shown in **Int3**. The HOMO of **Int3** (see Scheme 4) shows that the overlap between Ru and the MeOH proton is more favorable. Another situation is that the MeOH oxygen can attack the silylene ligand. Considering the lobe outside the Ru–Si bond is smaller than that inside the two $SiMe_2$ groups, we predict that the bonding between Ru and the hydrogen may be more favorable in between the two $SiMe_2$ groups than outside the Ru–Si bond. The second step (**Int1** to **Int2**) is the ring-opening of the four-membered ring.

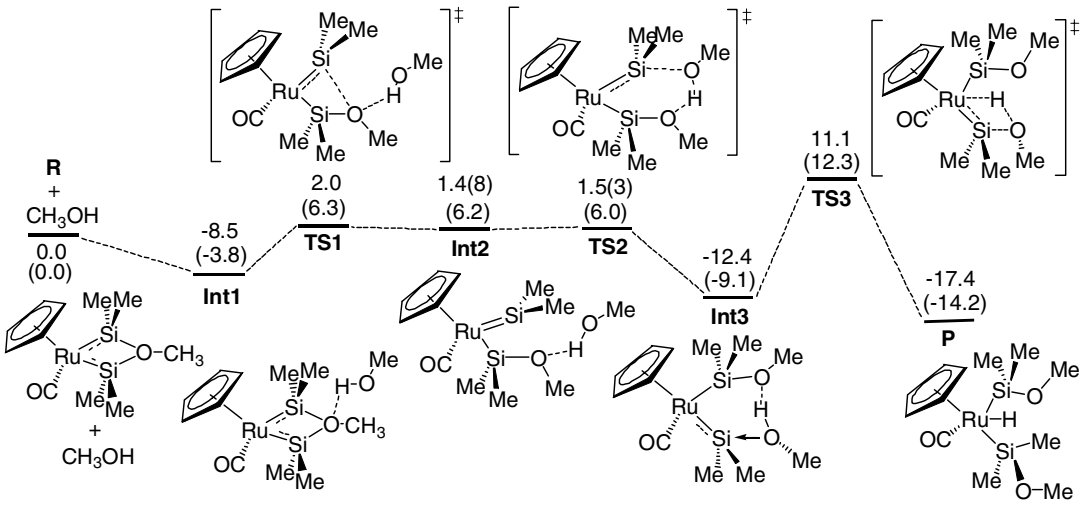

Fig. 1. Energy profile for reaction mechanism of Cp(CO)Ru{$SiMe_2$(OMe)$SiMe_2$} with MeOH. The relative energies are given in kcal/mol. The zero-point-energy corrected values are in parenthesis.

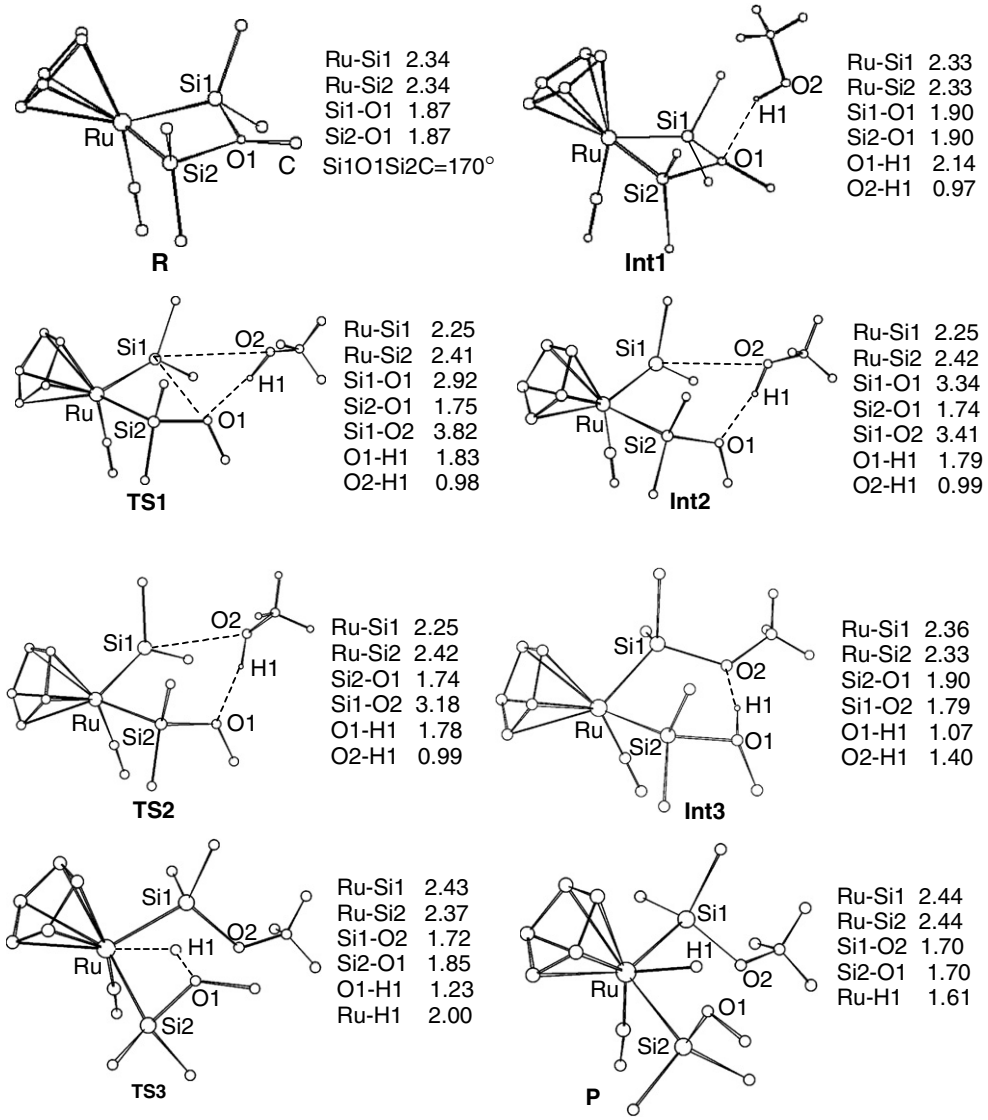

Fig. 2. Selected structural parameters (Å) calculated for the complexes shown in Fig. 1. For clarity, the hydrogen atoms on carbon atom are omitted.

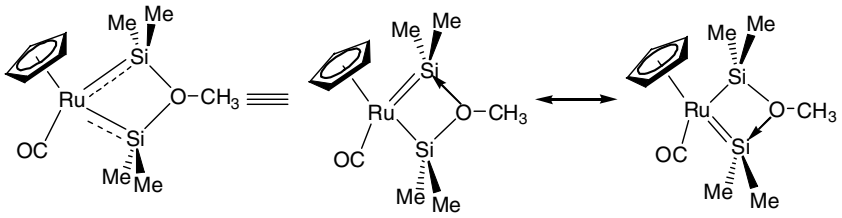

Scheme 3.

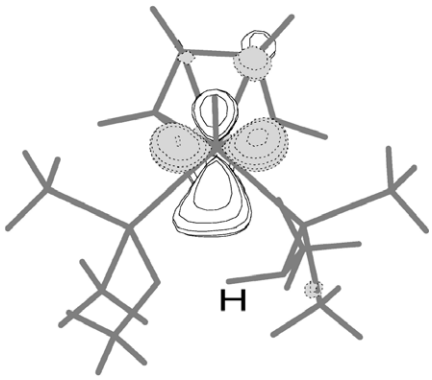

Scheme 4.

Accordingly, the O1···H1 hydrogen bonding is strengthened as a result of cleavage of the Si1–O1 bond. As Fig. 2 shows, the Si1–O1 bond changes from 1.90 Å in **Int1** to 3.34 Å in **Int2** and Si1···O2 distances are calculated to be 1.90 and 3.41 Å, respectively. The resonance disappears in **Int2** and the two Ru–Si bond lengths are no longer identical. Si1 is changed to have sp^2 hybridization and the Ru=Si1 double bond is formed. Si2 is changed to have sp^3 hybridization and the Ru–Si2 single bond is formed. Therefore, the Ru–Si1 becomes shorter and the Ru–Si2 longer compared with the case of **Int1**. The Si2–O1 bond transforms from a partial dative bond in **Int1** to a normal σ bond in **Int2** and hence the bond is strengthened. The Si2–O1 is calculated to be 1.74 Å in **Int2** while that is 1.90 Å in **Int1**. **TS1** is shown to be a late transition state. **Int2** is less stable than **Int1** due to the ring-opening where the conjugation formed by Ru, Si1, Si2, O1 is broken, indicating the bridging donor MeOH plays a role in stabilizing such kind of complexes by forming a four-membered ring of Ru–Si–O1–Si.

The third step is related to formation of a six-membered ring. Fig. 1 shows the activation barrier for the step is only 0.05 kcal/mol, but the Si1–O2 distance is apparently changed from 3.41 Å in **Int2** to 3.18 Å in **TS2**. The very low activation energy also suggests that this step is much favored kinetically. The hydroxyl O2 atom has a tendency to approach to Si1 and the hydroxyl H to O1 in **TS2**. IRC calculation confirms that the O2–H1 is smoothly elongated from **TS2** to **Int3**. As shown in **Int3**, the O2–H1 is lengthened to 1.40 Å and the O1–H1 is shortened to 1.07 Å, allowing the O1–H1 to be a σ bond and the O2–H1 interaction changing to be a hydrogen bond. As a result, the Si1–O2 mainly has σ bond character and the Si2–O1 mainly has dative-bond character. Therefore, the Si1–O2 is expected to be shorter than the Si2–O1. As confirmed by calculations, the former is 1.79 Å and the latter is 1.90 Å. It is easy to understand that the stronger the Si–O is, the weaker the Ru–Si is. Therefore, the Ru–Si2 is slightly shorter than the Ru–Si1 as a result of the fact that the Si1–O2 σ bond is stronger than the Si2–O1 dative bond. **Int3** is more stable than **Int2** mainly due to the enhanced interaction between Si1 and O2 compared with the situation in **Int2**.

The last step is the hydrogen migration from the hydroxyl oxygen to the metal center. Compared with **Int3**, the O2–H1 hydrogen bonding disappears in **TS3**, which makes the Si1–O2 bond stronger. Thus, the Si1 has sp^3 hybridization and correspondingly the Ru–Si1 is changed to be a completely single σ bond. Therefore this bond becomes longer than that in **Int3**. The O1–H1 is elongated to 1.23 Å and the Ru···H1 distance is 2.00 Å in **TS3**, indicating the H1 atom is moving from O1 to the metal center. The weaker O1–H1 makes the Si2–O1 bond stronger, and the Ru–Si2 bond is concertedly weaker. The barrier for the step is calculated to be 23.5 kcal/mol. The relatively high barrier seems to be understandable because this step involves breaking the strong O1–H1 bond. We attempted to locate a transition state which has lower activation energy, but **TS3** was always obtained. Although the barrier of 23.5 kcal/mol seems to be relatively high, the energy difference between **TS3** and (**R** + CH_3OH) is only 11.1 kcal/mol, consistent with the reaction condition to proceed at room temperature. In **P**, the hydrogen migration from O1 to Ru center affords a Ru–H1 bond. The two Ru–Si bonds become single σ bonds and have the same bond distance. The Ru–Si bond length (2.44 Å) is the longest among all the species involved in the reaction mechanism. Correspondingly, both the Si1–O2 and Si2–O1 become completely σ bonds and hence are the shortest among all species mentioned above. The hydrogen migration involved in the step can be understood through the HOMO of **Int3** as shown in Scheme 4. The lobe close to H in the HOMO is the largest, giving favorable overlapping with the migrating H atom. The charges on Ru and the H atom are −0.392 and +0.546, respectively, indicating that the electrostatic attraction between the two atoms is present. Therefore, the hydrogen migration becomes available. **P** is more stable than **Int3** by 5 kcal/mol, and is the most stable among all the species throughout the reaction mechanism. The driv-

ing force is the formation of the Ru–H and the normal Si–O σ bond.

For the overall reaction mechanism it can be seen from Fig. 1 that the rate-determining step is the hydrogen migration from the hydroxyl oxygen to the Ru center. The reaction energy difference is calculated to be −17.4 kcal/mol, indicating that the reaction is favorable thermodynamically.

3.2. Variation of structural parameters

Some systematic variations can be drawn from the structural parameters of the species discussed above, which is helpful to better understand the bonding involved in the reaction mechanism. Fig. 3 shows the variation of Ru–Si1 bond length with the change of Si1–O2 distance (a), and that of Ru–Si2 bond length with the change of Si2–O1 distance (b). As seen from Fig. 3a that the Ru–Si1 bond length decreases with the increase of Si1–O2 distance. In other words, the stronger the Si1–O2 is, the weaker the Ru–Si1 is. For **TS1**, the Ru–Si1 bond strength is affected not only by the Si1···O2 interaction but also by Si1–O1 interaction. So **TS1** are not included in the figure. It is found that a sharp decrease of the Ru–Si1 bond length occurs with the increase of Si1–O2 distance from **P** to **Int3** while a mild decrease exists from **Int3** to **Int2**. This is a result of strong interaction between Si1 and O2 in **Int3**, **TS3** and **P**. While in **TS2** and **Int2**, only a weak interaction is existent between Si1 and O2, which leads to the slight influence on the Ru–Si1 bond strength. In a word, if there exist a weak interaction between Si1 and O2, the variation of the Si1–O2 bond distance gives rise to the Ru–Si1 bond length changing mildly, and vice versa.

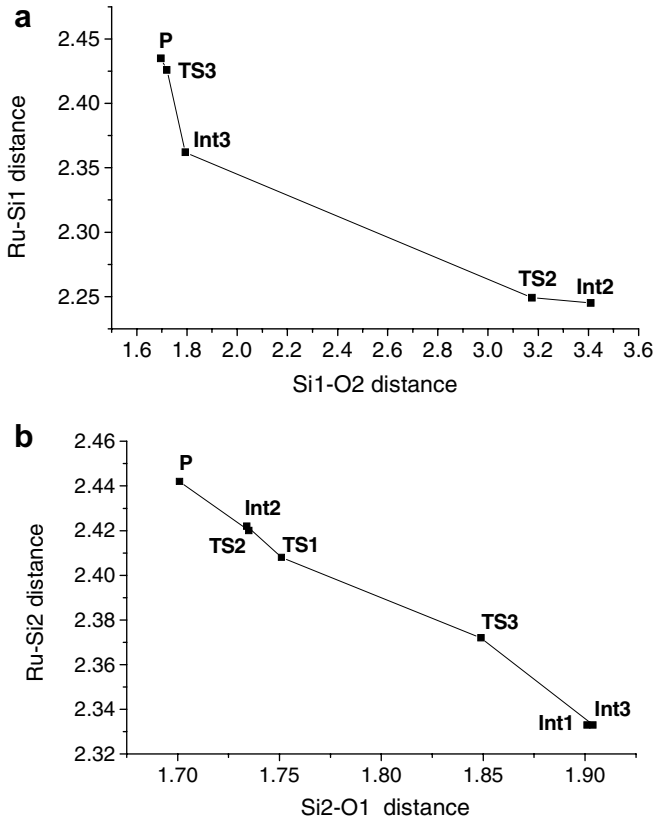

Fig. 3. Relationship between Ru–Si bond length and Si–O distance. (a) Ru–Si1 vs. Si1–O2 and (b) Ru–Si2 vs. Si2–O1.

TS1 is included in Fig. 3b, for the reason that the Ru–Si2 is mainly affected by strong Si2–O1 bond. The influence of the weak Si1···O1 and O1–H1 interactions on the bond strength of Ru–Si2 are negligible. Fig. 3b shows the Ru–Si2 bond length decreases smoothly with the increase of Si2–O1 bond length, indicating the Ru–Si2 bond strength increases with the decrease of the Si2–O1 bond strength. In contrast to Fig. 3a where an inflexion point (**Int3**) appears, no inflexion point is found in Fig. 3b. The difference between the two cases is that the weak Si1–O2 interaction is involved in (a), while only strong Si2–O1 is involved in (b). It can be found that the varying trend in (b) is similar to that in (a) from **Int3** to **Int2**, as a result of Si–O having strong interaction.

Some other structural parameters' variations can be seen from Table 1. Clearly, the O2–H1 is weakened with the stronger O1···H1 hydrogen bonding. The stronger the O1···H1 hydrogen bonding is, the weaker the Si2–O1 bond is.

3.3. Examination on the influence of hydrogen bonding

As seen from the reaction mechanism shown in Fig. 1, the reaction rate-determining step is the hydroxyl hydrogen migration from oxygen to Ru center. It is worth to note that the proposed reaction mechanism shown in Fig. 1 does not consider the influence of hydrogen bonding formed with other methanol molecules. In fact, hydrogen bonding is existent in the real reaction system. For exploring the influence of the hydrogen bonding on the reaction mechanism, we consider one more methanol molecule that forms a hydrogen bond with the species involved in the reaction. Now the most important is to focus the influence of hydrogen bonding on the rate-determining step. Fig. 4 shows the potential energy profile for the rate-determining step of the hydroxyl hydrogen migration which involves formation of hydrogen bonding. The values of the relative energies of $\mathbf{Int3_{MeOH}}$, $\mathbf{TS3_{MeOH}}$, and $\mathbf{P_{MeOH}}$ are obtained on the basis of defining the energy of (**R** + 2MeOH) as 0 kcal/mol. It is noted that the energy of "2MeOH" is not simply summation of the energies of two separate methanol molecules, but is calculated by putting them together where the hydro-

Table 1
Calculated bond distances of the O2–H1, H1···O1, O1–Si2, O2–Si1 in **Int1**, **TS2**, and **Int2**

	Int1	TS1	Int2	TS2	Int3
O2–H1	0.97	0.98	0.99	0.99	1.07
O1···H1	2.13	1.83	1.79	1.78	1.40
O1–Si2	1. 90	1.75	1.74	1.74	1.90

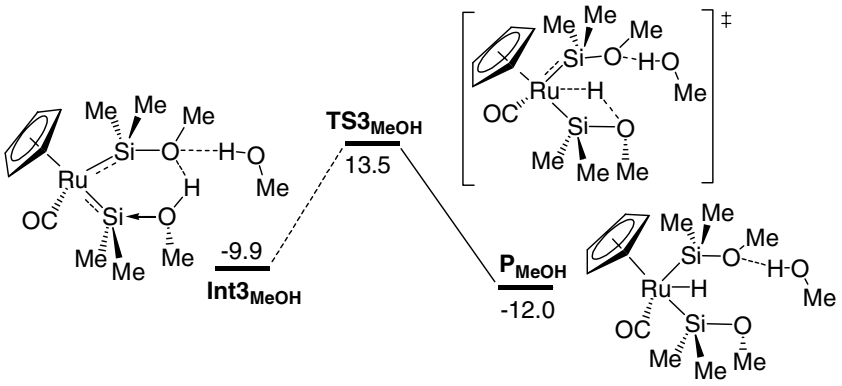

Fig. 4. Potential energy profile for the rate-determining step of the hydroxyl hydrogen migration, considering the hydrogen bonding. The relative energies given in kcal/mol are obtained relative to (**R** + 2MeOH). The energy of (**R** + 2MeOH) is defined as 0 kcal/mol.

gen bonding between them occurs. In $\mathbf{Int3_{MeOH}}$, results of calculations show that a hydrogen bond is formed between O2···H2 (2.04 Å). Clearly, the occurrence of the O2···H2 hydrogen bonding weakens the O2···H1 hydrogen bonding, leading to the O2···H1 distance increased by 0.09 Å and accordingly the O1–H1 bond length decreased by 0.03 Å relative to the corresponding data in **Int3**. The other bond distances are almost similar to those in **Int3**. In $\mathbf{TS3_{MeOH}}$ and $\mathbf{P_{MeOH}}$, the O2···H2 hydrogen bonds are still remained. The migration of the hydroxyl hydrogen from O1 to Ru is analogous to the case without considering the hydrogen bonding.

It can be drawn as follows from comparing the rate-determining step from $\mathbf{Int3_{MeOH}}$ via $\mathbf{TS3_{MeOH}}$ to $\mathbf{P_{MeOH}}$ in Fig. 4 and the one from **Int3** via **TS3** to **P** in Fig. 1. (1) The activation barrier for the rate-determining step with the hydrogen bonding considered (23.4 kcal/mol) is calculated to be almost the same as that without considering the hydrogen bonding (23.5 kcal/mol), implying that the hydrogen bonding hardly affects the activation barrier for the rate-determining step. (2) The three species in Fig. 4 are not lowered in energy but slightly increased compared with the three corresponding species in Fig. 1. The reason may be that the hydrogen bonding involved in the intermediates and the transition states is weaker than that formed in the two methanol molecules in (**R** + 2MeOH). The highest barrier relative to the reactants is hence increased a little (13.5 − 11.1 = 2.4 kcal/mol). That means the occurrence of hydrogen bonding does not lower but slightly heighten the reaction barrier (Fig. 5).

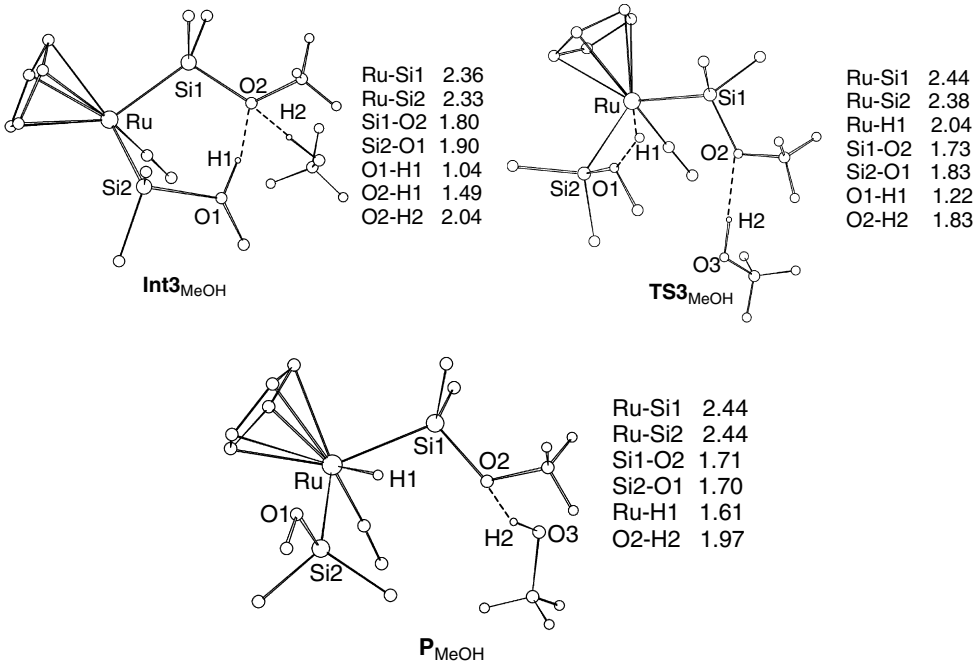

Fig. 5. B3LYP optimized geometric structures with selected structural parameters (Å) for the three species shown in Fig. 4. For clarity, the hydrogen atoms on carbon atoms are omitted except for those introduced by the two methanol molecules.

4. Conclusion

In this paper, the mechanism on formation of Cp(OC)Ru(H)($SiMe_2OMe)_2$ from $CpRu(CO)_2SiMe_2SiMe_2OR$ and MeOH has been theoretically investigated with the aid of density functional theory calculations. Four steps are involved in the reaction (formation of hydrogen bonding between **R** and a MeOH, ring-opening of the Ru–Si1–O1–Si2 four-membered ring, formation of the six-membered ring, and the hydroxyl hydrogen migration to the metal center). The hydroxyl hydrogen migration from hydroxyl oxygen to Ru center is found to be the rate-determining step. The reaction is calculated to be favorable thermodynamically. Our results of calculations are consistent with the experimental observation that Cp(OC)Ru{$SiMe_2(OMe)SiMe_2$} (**R**) reacts with MeOH to afford the product Cp(OC)Ru(H)($SiMe_2OMe)_2$ (**P**) cleanly. In addition, systematic parameter variations among Ru–Si, Si–O and Si···H are analyzed. The varying trends tell that the Ru–Si bond length is strengthened with the weakening of the Si···O interaction. It is also found by further insight into the parameter variations that the influence of weak Si1···O2 interaction on Ru–Si1 bond strength is different from the influence of the strong Si2···O1 interaction on the Ru–Si2 bond strength. We hope that the mechanistic study, on the reactions of alkoxy-bridged bis(silylene) transition-metal complexes toward some small nucleophilic agents such as MeOH, can provide deep understanding for theoretical and experimental chemists.

Acknowledgement

This work was supported by the National Science Foundation of China (No. 20473047).

References

[1] D.A. Straus, T.D. Tilley, J. Am. Chem. Soc. 109 (1987) 5872.
[2] (a) C. Zybill, G. Muller, Angew. Chem., Int. Ed. Engl. 26 (1987) 669;
(b) C. Zybill, G. Muller, Organometallics 7 (1988) 1368;
(c) C. Zybill, D.L. Wilkinson, G. Muller, Angew. Chem., Int. Ed. Engl. 27 (1988) 583;
(d) C. Zybill, D.L. Wilkinson, C. Leis, G. Muller, Angew. Chem., Int. Ed. Engl. 28 (1989) 203.
[3] K. Ueno, H. Tobita, M. Shimoi, H. Ogino, J. Am. Chem. Soc. 110 (1988) 4092.
[4] (a) H. Tobita, H. Wada, K. Ueno, H. Ogino, Organometallics 13 (1994) 2545;
(b) H. Tobita, K. Ueno, M. Shimoi, H. Ogino, Organometallics 112 (1990) 3415.
[5] T. Tamiko, H. Tobita, H. Ogino, Organometallics 10 (1991) 835.
[6] K. Ueno, A. Masuko, H. Ogino, Organometallics 18 (1999) 2694.
[7] K. Ueno, A. Masuko, H. Ogino, Organometallics 16 (1997) 5023.
[8] H. Jacobsen, T. Ziegler, Inorg. Chem. 35 (1996) 775.
[9] Maria Besora, Feliu Maseras, Agustı'Lledo Odile Eisenstein, Organometallics 25 (2006) 4748.
[10] D.S. McGuinness, B.F. Yates, K.J. Cavell, Organometallics 21 (2002) 5408.
[11] J.Y. Corey, J. Braddock-Wilking, Chem. Rev. 99 (1999) 75.
[12] C.H. Suresh, N. Koga, Organometallics 20 (2001) 4333.
[13] (a) M.-F. Fan, G. jia, Z. Lin, J. Am. Chem. Soc. 118 (1996) 9915;
(b) K.Yu. Dorogov, E. Dumont, N.-N. Ho, A.V. Churakov, L.G. Kuzmina, J.-M. Poblet, A.J. Schultz, J.A.K. Howard, R. Bau, A. Lledos, G.I. Nikonov, Organometallics 23 (2004) 2845;
(c) K.K. Pandey, M. Lein, G. Frenking, Organometallics 23 (2004) 2944.
[14] (a) M. Ray, Y. Nakao, H. Sato, S. Sakaki, Organometallics 26 (2007) 4413;
(b) J.M. Jasinski, R. Becerra, R. Walsh, Chem. Rev. 95 (1995) 1203.
[15] K. Ueno, S. Ito, H. Tobita, S. Inomata, H. Ogino, Organometallics 13 (1994) 3309.
[16] H. Nakazawa, Y. Miyoshi, T. Katayama, T. Mizuta, K. Miyoshi, N. Tsuchida, A. Ono, K. Takano, Organometallics 25 (2006) 5913.
[17] X. Zhu, B. Zhao, B. Wang, S. Bi, Chem. Phys. Lett. 422 (2006) 6.
[18] S.R. Klei, T.D. Tilley, R.G. Bergman, Organometallics 21 (2002) 4648.
[19] M. Okazaki, H. Tobita, H. Ogino, Dalton Trans. (2003) 493.
[20] H. Wada, H. Tobita, H. Ogino, Organometallics 16 (1997) 2200.
[21] K. Ueno, H. Tobita, S. Seki, H. Ogino, Chem. Lett. 10 (1993) 1723.
[22] H. Tobita, H. Kurita, H. Ogino, Organometallics 17 (1998) 2844.
[23] C. Lee, W. Yang, G. Parr, Phys. Rev. B 37 (1988) 785.
[24] A.D. Becke, J. Chem. Phys. 98 (1993) 5648.
[25] P.J. Hay, W.R. Wadt, J. Chem. Phys. 82 (1985) 270.
[26] W.R. Wadt, P.J. Hay, J. Chem. Phys. 82 (1985) 284.
[27] P.J. Hay, W.R. Wadt, J. Chem. Phys. 82 (1985) 299.
[28] P.C. Hariharan, J.A. Pople, Theor. Chim. Acta 28 (1973) 213.
[29] R.C. Binning Jr., L.A. Curtiss, J. Comput. Chem. 11 (1990) 1206.
[30] M.S. Gordon, Chem. Phys. Lett. 76 (1980) 163.
[31] W.J. Hehre, L. Radom, P.V.R. Schleyer, J.A. Pople, Abinitio Molecular Orbital Theory, Wiley, New York, 1986.
[32] S. Huzinaga, Gaussian Basis Sets for Molecular Calculations, Elsevier Science, Amsterdam, 1984.
[33] C. Gonzalez, H.B. Schlegel, J. Chem. Phys. 94 (1990) 5523.
[34] C. Gonzalez, H.B. Schlegel, J. Chem. Phys. 90 (1989) 2154.
[35] M.J. Frisch, G.W. Trucks, H.B. Schlegel, G.E. Scuseria, M.A. Robb, J.R. Cheeseman, V.G. Zakrzewski, J.A. Montgomery Jr., R.E. Stratmann, J.C. Burant, S. Dapprich, J.M. Millam, A.D. Daniels, K.N. Kudin, M.C. Strain, O. Farkas, J. Tomasi, V. Barone, M. Cossi, R. Cammi, B. Mennucci, C. Pomelli, C. Adamo, S. Clifford, J. Ochterski, G.A. Petersson, P.Y. Ayala, Q. Cui, K. Morokuma, D.K. Malick, A.D. Rabuck, K. Raghavachari, J.B. Foresman, J. Cioslowski, J.V. Otitz, B.B. Stefanov, G. Liu, A. Liashenko, P. Piskorz, I. Komaromi, R. Gomperts, R.L. Martin, D.J. Fox, T. Keith, M.A. Al-Laham, C.Y. Peng, A. Nanayakkara, C. Gonzales, M. Challacombe, P.M.W. Gill, B. Johnson, W. Chen, M.W. Wong, J.L. Andres, M. Head-Gordon, E.S. Replogle, J.A. Pople, GAUSSIAN 98 Revision A.5, Gaussian Inc., Pittsburgh, PA, 1998.
[36] S. Niu, M.B. Hall, Chem. Rev. 100 (2000) 353.
[37] J. Zhu, G. Jia, Z. Lin, Organometallics 25 (2006) 1812.
[38] S. Bi, Z. Lin, R.F. Jordan, Organometallics 23 (2004) 4882.
[39] S. Bi, S. Zhu, Z. Zhang, Z. Yuan, J. Organomet. Chem. 692 (2007) 3454.
[40] S. Bi, A. Ariafard, G. Jia, Z. Lin, Organometallics 24 (2005) 680.
[41] P. Xue, S. Bi, H. Herman, Y. Sung, I.D. Williams, Z. Lin, G. Jia, Organometallics 23 (2004) 4735.
[42] S. Bi, S. Zhu, Z. Zhang, Eur. J. Inorg. Chem. 14 (2007) 2046.
[43] G. Schaftenaar, MOLDEN v3.5, CAOS/CAMM Center Nijmegen, Toernooiveld, Nijmegen, The Netherlands, 1999.